Repeated interaction model for diffusion-induced Ramsey narrowing

Yanhong Xiao [1], Irina Novikova [2], David F. Phillips [1], Ronald L. Walsworth [1,3]

[1] *Harvard-Smithsonian Center for Astrophysics, Cambridge, Massachusetts, 02138*
[2] *The College of William and Mary, Williamsburg, Virginia, 23187*
[3] *Department of Physics, Harvard University, Cambridge, Massachusetts, 02138*

yxiao@post.harvard.edu

Abstract: In a recent paper [Y. Xiao *et al.*, Phys. Rev. Lett. **96**, 043601 (2006)] we characterized diffusion-induced Ramsey narrowing as a general phenomenon, in which diffusion of coherence in-and-out of an interaction region such as a laser beam induces spectral narrowing of the associated resonance lineshape. Here we provide a detailed presentation of the repeated interaction model of diffusion-induced Ramsey narrowing, with particular focus on its application to Electromagnetically Induced Transparency (EIT) of atomic vapor in a buffer gas cell. We compare this model both to experimental data and numerical calculations.

OCIS codes: (020.1670) Atomic and molecular physics : Coherent optical effects;
(020.3690) Atomic and molecular physics : Line shapes and shifts;
(030.1640) Coherence and statistical optics : Coherence;
(300.3700) Spectroscopy : Linewidth;
(270.1670) Quantum optics : Coherent optical effects.

References and links

1. W. Happer, "Optical pumping," Rev. Mod. Phys. **44,** 169–249 (1972).
2. E. Arimondo, "Relaxation processes in coherent-population trapping," Phys. Rev. A **54**, 2216–2223 (1996).
3. M. Erhard and H. Helm, "Buffer-gas effects on dark resonances: theory and experiment," Phys. Rev. A **63**, 043813 (2001).
4. Y. Xiao, I. Novikova, D. F. Phillips and R. L. Walsworth, "Diffusion-induced Ramsey narrowing," Phys. Rev. Lett. **96**, 043601 (2006).
5. N. F. Ramsey, *Molecular beams* (Clarendon, Oxford, 1956).
6. A. S. Zibrov, I. Novikova and A. B. Matsko, "Observation of Ramsey fringes in an atomic cell with buffer gas," Opt. Lett. **26**, 1311–1313 (2001).
7. A. S. Zibrov and A. B. Matsko, "Optical Ramsey fringes induced by Zeeman coherence," Phys. Rev. A **65**, 013814 (2001).
8. E. Alipieva, S. Gateva, E. Taskova, and S. Cartaleva, "Narrow structure in the coherent population trapping resonance in rubidium," Opt. Lett. **28**, 1817–1819 (2003).
9. G. Alzetta, S. Carta1eva, S. Gozzini, T. Karaulanov, A. Lucchesini, C. Marinelli, L. MOi, K. Nasyrov, V. Sarova, K. Vaseva, "Magnetic Coherence Resonance Profiles in Na and K," Proc. SPIE, **5830**, 181–185 (2005).
10. J. Vanier, "Atomic clocks based on Coherent Population Trapping: a review," Appl. Phys. B **81**(4), 421–442 (2005).
11. D. Budker, W. Gawlik, D. F. Kimball, S. M. Rochester, V. V. Yashchuk, and A. Weis, "Resonant nonliear magneto-optical effects in atoms," Rev. Mod. Phys. **74**, 1153–1201 (2002).
12. I. Novikova, Y. Xiao, D. F. Phillips, and R. L. Walsworth,"EIT and diffusion of atomic coherence," J. Mod. Opt., **52**, 2381–2390 (2005).
13. M. D. Lukin, "Colloquium: Trapping and manipulating photon states in atomic ensembles," Rev. Mod. Phys. **75**, 457–472 (2003).

#97131 - $15.00 USD Received 6 Jun 2008; revised 1 Aug 2008; accepted 4 Aug 2008; published 26 Aug 2008

14. T. Zanon, S. Guerandel, E. de Clercq, D. Holleville, N. Dimarcq, and A. Clairon, "High contrast Ramsey fringes with Coherent-Population-Trapping pulses in a double lambda atomic system," Phys. Rev. Lett. **94**, 193002 (2005).
15. M. O. Scully, and M. S. Zubairy, *Quantum Optics* (Cambridge University Press, Cambridge, UK, 1997).
16. M. S. Shahriar, P. R. Hemmer, D. P. Katz, A. Lee and M. G. Prentiss, "Dark-state-based three-element vector model for the stimulated Raman interaction," Phys. Rev. A **55**, 2272–2282 (1997).
17. F. Levi, A. Godone, J. Vanier, S. Micalizio, and G. Modugno, "Line-shape of dark line and maser emission profile in CPT," Eur. Phys. J. D **12**, 53 (2000).
18. A. V. Taichenachev, A. M. Tumaikin, V. I. Yudin, M. Stahler, R. Wynands, J. Kitching, and L. Hollberg,"Nonliear-resonance line shapes: Dependence on the transverse intensity distribution of a light beam," Phys. Rev. A **69**, 024501 (2004).
19. E. Pfleghaar, J. Wurster, S. I. Kanorsky and A. Weis, "Time of flight effects in nonliear magneto-optical spectroscopy," Optics Commun. **99**, 303–308 (1993).
20. P. R. Hemmer, M. S. Shahriar, V. D. Natoli, and S. Ezekiel,"AC Stark shifts in a two-zone Raman interaction," J. Opt. Soc. Am. B **6**, 1519–1528 (1989).
21. M. D. Lukin, M. Fleischhauer, A. S. Zibrov, H. G. Robinson, V. L. Velichansky, L. Hollberg and M. O. Scully, "Spectroscopy in dense coherent media: Line narrowing and interference effects," Phys. Rev. Lett. **79**, 2959–2962 (1997).
22. J. Vanier, M. W. Levine, D. Janssen, M. Delaney, "Contrast and linewidth of the coherent population trapping transmission hyperfine resonance line in ^{87}Rb : Effect of optical pumping," Phys. Rev. A. **67**, 065801 (2003).
23. *Numerical recipies in C: the art of scientific computing, second edition*, W. H. Press, S. A. Teukolsky, W. T. Vetterling, B. P. Flannery, Cambridge University Press, New York (1992) Ch. 19.
24. A typical EIT lineshape, such as that shown in figure 7, takes approximately 12 hours to calculate on a 1.25 GHz PowerPC G4 whereas the repeated interaction model can be evaluated immediately.
25. W. Zhang and D. G. Cory, "First Direct Measurement of the Spin Diffusion Rate in a Homogenous Solid," Phys. Rev. Lett. **80**, 1324–1327 (1998).
26. For example, the interplay of spin diffusion with electron-spin-mediated nuclear-spin coherence may play a critical role in recent measurements in quantum dots; private communication, J. Taylor.
27. J. Petta, A. C. Johnson, J. M. Taylor, E. A. Laird, A. Yacoby, M. D. Lukin, C. M. Marcus, M. P. Hanson , A. C. Gossard, "Coherent manipulation of coupled electron spins in semiconductor quantum dots," Science **309**, 2180–2184 (2005).

1. Introduction

Atomic motion can affect the lineshape of an atomic transition. For example, transit-time broadening often sets a limit on the narrowest linewidth obtainable in the interaction of a thermal atomic vapor with a collimated laser beam. In the case of Electromagnetically Induced Transparency (EIT) for an atomic vapor constrained to diffuse in a buffer gas which only weakly perturbs ground state coherence in a collision, the interaction time is usually estimated by the lowest order diffusion mode, which leads to the typical Lorentzian lineshape but implicitly assumes that atoms diffuse out of the laser beam and do not return [1, 2, 3]. In recently published work [4] we characterized an important but heretofore overlooked line narrowing process — "diffusion-induced Ramsey narrowing" — in which atoms diffuse out of the interaction region and return before decohering. In this process, atoms evolve coherently in the dark (outside of the laser beam) between periods of interaction (inside the laser beam), in analogy to Ramsey spectroscopy [5]. See Fig. 1. In many cases of interest, diffusing atoms can spend a majority of their coherence lifetime in the dark, which induces a significant spectral narrowing of the center of the atomic lineshape, making it distinctly non-Lorentzian [6, 7, 8, 9]. An example measurement of this phenomenon is shown in Fig. 2 for the case of EIT in Rb vapor.

Detailed, quantitative understanding of such non-Lorentzian lineshapes is necessary in a variety of applications including atomic frequency standards [10], precision metrology [1, 10, 11, 12] and nonlinear light-matter interactions such as slow and stored light [13]. In particular, over wide ranges of laser intensity, beam diameter, and buffer gas pressure, EIT lineshapes are found to differ both quantitatively and qualitatively from expectations based on the lowest order diffusion mode. See Fig. 2. In our previous paper [4] we presented a brief description of the "repeated interaction model," an intuitive analytical model of the repeated diffusive re-

#97131 - $15.00 USD Received 6 Jun 2008; revised 1 Aug 2008; accepted 4 Aug 2008; published 26 Aug 2008

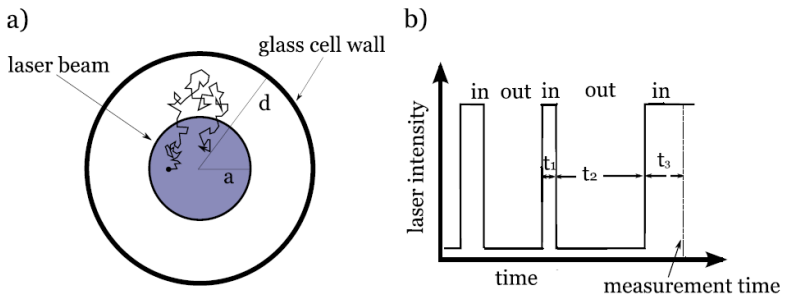

Fig. 1. (a) Cross-section schematic of a vapor cell showing the vapor cell wall at $r = d$, a step-like laser beam of radius a, and a cartoon of an atom's random walk in, out, and back into the laser beam. (b) Atoms diffusing in and out of the laser beam experience a Ramsey-like sequence of alternating periods of interaction with the laser fields and evolution in the dark. The simplest in-out-in Ramsey sequence is indicated with the corresponding times t_1, t_2, and t_3.

turn of atomic coherence to the interaction region, which allows straightforward calculation of the effects of diffusion-induced Ramsey narrowing in good agreement with a wide range of experimental conditions. Here we present a more detailed treatment of this model and its application to EIT in atomic vapor, including a comparison to experimental data and numerical calculations. The repeated interaction model decouples the random motion of atoms from their dynamic response to the EIT laser fields, reducing computational complexity and allowing for an analytical solution. In outline, the model consists of (i) solving the time evolution of the atomic density matrix as a function of the history ("Ramsey sequence") of time spent in and out of the laser beam (See Fig. 1b); (ii) evaluating the probability distributions for the in and out periods from the underlying diffusion equation; and (iii) integrating the density matrix solutions over the probability distributions to determine the ensemble average lineshape.

2. Repeated interaction model

2.1. Atomic density matrix following a Ramsey sequence

EIT results from optical pumping of atoms into a noninteracting dark state for two optical fields (often two spectral components of a single laser beam) that are in two-photon Raman resonance with a pair of metastable ground states of the atomic system [15]. EIT gives rise to a narrow transmission resonance for the optical fields, with a minimum spectral width set by the rate of decoherence between the two ground states constituting the dark state. As shown in our recent paper [4], EIT lineshapes can be greatly affected by diffusion-induced Ramsey narrowing.

Here we consider a general 3-level Λ system for EIT in an optically thin medium, as shown in Fig. 3. Two laser fields with frequencies ω_p and ω_d and Rabi frequencies (defined in the same way as in [16]) Ω_P (probe beam) and Ω_D (drive beam) couple two ground electronic states (typically hyperfine levels) to an electronically excited state: $|a\rangle \rightarrow |e\rangle$ and $|b\rangle \rightarrow |e\rangle$, respectively. The excited state decays to the two ground states with equal rate $\gamma/2$. The ground state population difference and coherence each relax to zero with a rate Γ_0 (including residual magnetic field inhomogeneity and spin exchange etc., but not including effects of optical pumping and collision with the cell walls). A step-like cylindrical laser profile is assumed (see See Fig. 1a) to ease computation and isolate diffusion-induced spectral reshaping from effects due to the transverse variation of the laser beam profile [17, 18, 19]. In Sec. 4 below we provide numerical comparisons between step-like and Gaussian laser beam profiles to study the role of

#97131 - $15.00 USD Received 6 Jun 2008; revised 1 Aug 2008; accepted 4 Aug 2008; published 26 Aug 2008

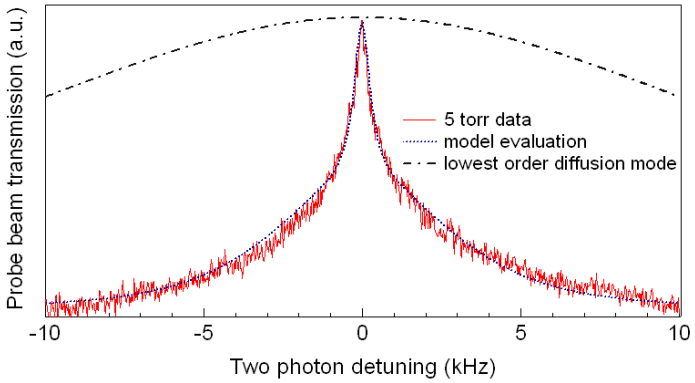

Fig. 2. Comparison of experimental data for the EIT lineshape in Rb vapor with predictions from the repeated interaction model and a simple Lorentzian lineshape with width given by the lowest order mode for atomic diffusion out of the laser beam. Red solid line: experimental data for a Rb vapor cell with 5 torr Ne buffer gas and a laser beam with 22 μW power and a Gaussian transverse profile with 0.8 mm separation between half-intensity points. Blue dotted line: prediction from the repeated interaction model for a step-like laser beam with 0.96 mm diameter, 30 cm^2/s Rb diffusion coefficient [12], $2\pi \times 95$ kHz Rabi frequency of the drive field, 100 MHz FWHM excited state linewidth, and 100 Hz FWHM groundstate linewidth). Black dotted-dashed line: Lorentzian lineshape with width given by the lowest order diffusion mode for a laser beam with 0.8 mm diameter and 30 cm^2/s Rb diffusion coefficient. In all cases, EIT peak amplitude and baseline offset have been scaled to match data.

beam profiles in the repeated interaction model.

The probe field absorption and transmission are given by the imaginary part of the off-diagonal matrix element ρ_{ea}, which for an optically thin medium is homogeneous along the longitudinal axis of the atomic ensemble and laser beam. In the appendix we derive the atomic density matrix for the simplest Ramsey sequence in which an atom spends time t_1 in the laser beam, evolves freely in the the dark for time t_2, and then re-enters the laser beam for time t_3 (see Fig. 1b). We assume that the drive field is resonant with the $|a\rangle \rightarrow |e\rangle$ transition, the probe field is near resonance with the $|b\rangle \rightarrow |e\rangle$ transition, the ratio of probe to drive Rabi frequencies is small, and the overall intensity of all optical fields is weak enough that the excited state can be adiabatically eliminated. Then the imaginary part of ρ_{ea} following the above Ramsey sequence has a relatively simple form:

$$\begin{aligned}\frac{\mathrm{Im}\left(\rho_{ea}\right)}{\Omega_P} = & \\ & \frac{\alpha_D}{\left(\Delta^2+\Gamma^2\right)\gamma^2}\cdot \mathrm{Re}\left\{\left[\gamma\Gamma-\Delta^2+i\Delta\left(\gamma+\Gamma\right)\right]\right. \\ & \left.\left(-1+e^{-t_3(\Gamma-i\Delta)}-e^{-t_3(\Gamma-i\Delta)-t_2(\Gamma_0-i\Delta)}+e^{-(t_1+t_3)(\Gamma-i\Delta)-t_2(\Gamma_0-i\Delta)}\right)\right\} \\ & -\frac{\alpha_D}{2\Gamma\gamma}\cdot\left(-1+e^{-t_3\Gamma}-e^{-t_3\Gamma-t_2\Gamma_0}+e^{-(t_1+t_3)\Gamma-t_2\Gamma_0}\right)+\frac{1}{2\gamma}\end{aligned} \tag{1}$$

where $\alpha_D = \Omega_D^2/2\gamma$ is the optical pumping rate, $\Gamma = \alpha_D + \Gamma_0$, and Δ is the two-photon detuning. This result follows from Eq. (16) of the appendix in the limit $\gamma \gg \Delta$ relevant to EIT experiments discussed here. One can extend Eq. (1) to Ramsey sequences consisting of an arbitrary number of dark periods, noticing that terms associated with various time periods simply form a power

#97131 - $15.00 USD Received 6 Jun 2008; revised 1 Aug 2008; accepted 4 Aug 2008; published 26 Aug 2008

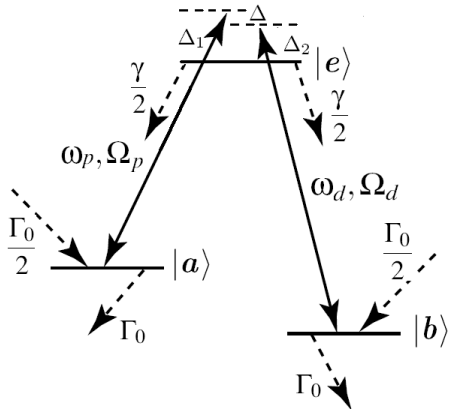

Fig. 3. Three-level Λ system coupled by probe and drive fields with one-photon detunings $\Delta_1 = \omega_p - \omega_{ea}$ and $\Delta_2 = \omega_d - \omega_{eb}$, respectively. Two-photon detuning: $\Delta = \Delta_1 - \Delta_2$. Average one-photon detuning: $\delta = (\Delta_1 + \Delta_2)/2$.

series.

Three distinct regimes of EIT can be represented by Eq. (1) in different limits: (a) "equilibrium EIT," in which atoms spend a long time in the laser beam and come into equilibrium with the laser fields, given by the limit $t_1 = t_2 = 0$ and $t_3 >> 1/\Gamma$; (b) "transit-time-limited EIT," in which atoms leave the beam before equilibrating with the laser fields and do not return before decohering, given by the limit $t_1 = t_2 = 0$ and $t_3 <\approx 1/\Gamma$; and (c) "Ramsey EIT," in which there is significant return of atomic coherence to the laser beam after evolution in the dark, given for the general case with t_1, t_2 and t_3 all being nonzero. As seen from Eq. (1), $e^{-t_3\Gamma} \approx 0$ for equilibrium EIT, which leads to a Lorentzian lineshape with halfwidth of Γ. Transit-time-limited EIT has a sinc-function lineshape (dashed curve of Fig. 4), with a period of $1/t_3$. Such lineshapes are observed in atomic beam experiments; however, the distribution of times spent in the laser beam for a steady-state vapor cell measurement washes out all but the central sinc-function lobe, as discussed below. The Ramsey EIT lineshape has a transit-time-limited envelope with underlying fringes, as shown by the solid curve of Fig. 4. The envelope has a width of $1/t_3$ and a fringe width of $1/t_2$. The fringes are caused by differential phase evolution of the atomic coherence for times spent inside and outside the laser beam. Similar lineshapes have been observed previously in pulsed-laser-beam vapor cells [14] and atomic beam experiments [20]. While the fringes are largely washed out in the Ramsey EIT lineshape of an atomic vapor cell, as discussed below, their effect remains in the narrow central EIT peak.

2.2. Probability distributions for Ramsey sequences

In an atomic vapor cell with buffer gas, the time an atom spends in and out of the laser beam is described by a distribution determined by the diffusion equation. We use $P(t_1,t_2,t_3)$ to denote the probability density of atoms that have an interaction history of being in the beam for a period t_1, then outside for t_2, and then back in the beam for t_3. Distributions of dark and bright times are independent so

$$P(t_1,t_2,t_3) = P_{\rm in}(t_1)P_{\rm out}(t_2)P_{\rm in}(t_3) \tag{2}$$

where $P_{\rm in}(t_1)$ and $P_{\rm out}(t_2)$ are the probability for an atom to continuously stay in and out of the beam for t_1 and t_2, etc. In general, the radial symmetry of both the vapor cell and the laser beam allows for a solution for $P_{\rm in}$ and $P_{\rm out}$ in cylindrical coordinates. Atom collisions with the cell walls are assumed to destroy all coherence between the ground states. For simplicity, the

#97131 - $15.00 USD Received 6 Jun 2008; revised 1 Aug 2008; accepted 4 Aug 2008; published 26 Aug 2008

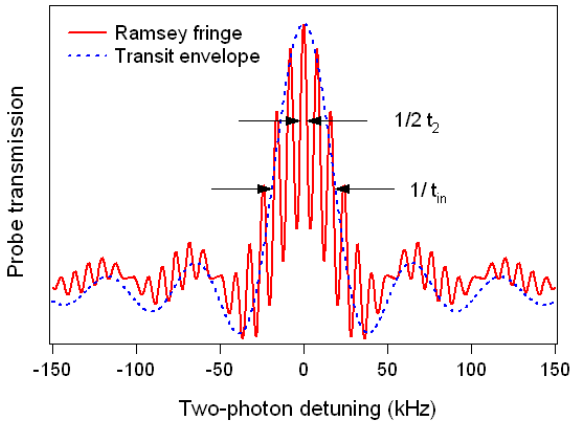

Fig. 4. Ramsey-EIT (solid line) calculated for a particular history (Ramsey sequence) with $t_1 = t_3 = \tau_D$ and $t_2 = 5\,\tau_D$, where $\tau_D = 19$ μs, $1/\tau_D = 52$ kHz, $\alpha_D = 2\pi \times 6.5$ kHz, $\Gamma_0 = 2\pi \times 50$ Hz, $\gamma = 2\pi \times 50$ MHz. The transit-time-limited envelope (dashed line) is calculated with $t_1 = t_2 = 0$, $t_3 = \tau_D$.

longitudinal (z-axis) boundary is assumed to be at infinity, reducing the problem to the radial variable r only.

We solved the diffusion equation analytically for the probability density $P(r,t)$ for atoms not to have diffused beyond radius r in time t. We then calculated $P_{\rm in}(t) = \int_{\rm beam} P(r,t)\,2\pi r dr$ with the initial condition of a uniform distribution, $P(r,0) = 1/(\pi a^2)$ for $r < a$ where a is the laser beam diameter; and the boundary condition $P(r = a,t) = 0$ to eliminate atoms that diffuse out of the beam. Integrating over the atoms remaining in the beam at time t gives the probability density,

$$P_{\rm in}(t) = 4\sum_{m=1}^{\infty} \frac{1}{\chi_m^2} \cdot e^{-(\frac{\chi_m}{2})^2 \cdot \frac{t}{\tau_D}} \tag{3}$$

where $\tau_D = a^2/4D$ (the lowest order diffusion mode in two dimensions), D is the atomic diffusion coefficient, and χ_m is the *mth* zero of J_0, the zeroth Bessel function of the first kind. For $t > \approx \tau_D$, the lowest order mode dominates this distribution. Note that the distribution of times inside the beam with times measured in units of the lowest order diffusion mode $\tilde{t}_{\rm in} = t/\tau_D$ is independent of any geometric or diffusion parameters. The dashed line in Fig. 5a shows $P_{\rm in}(\tilde{t}_{\rm in})$ as determined from Eq. (3).

An approximate analytical solution to $P_{\rm out}(t)$, the distribution of times spent out of the beam, can be found using the "small beam approximation" in which we assume that the laser beam cross-section is much smaller than the cell diameter. In this approximation, an atom spends negligible time in the laser beam. $P_{\rm out}(t)$ is then approximated as the probability that an atom, starting in the laser beam at time zero, is again in the laser beam at t. Because atoms spend little time in the beam, we assume that it was outside the beam for the entire period. This approximation leads to

$$P_{\rm out}(t) = 4\sum_{m=1}^{\infty} e^{-\frac{D\chi_m^2 t}{d^2}} \frac{J_1\left(\frac{a\chi_m}{d}\right)^2}{\chi_m^2 J_1(\chi_m)^2}. \tag{4}$$

#97131 - $15.00 USD Received 6 Jun 2008; revised 1 Aug 2008; accepted 4 Aug 2008; published 26 Aug 2008

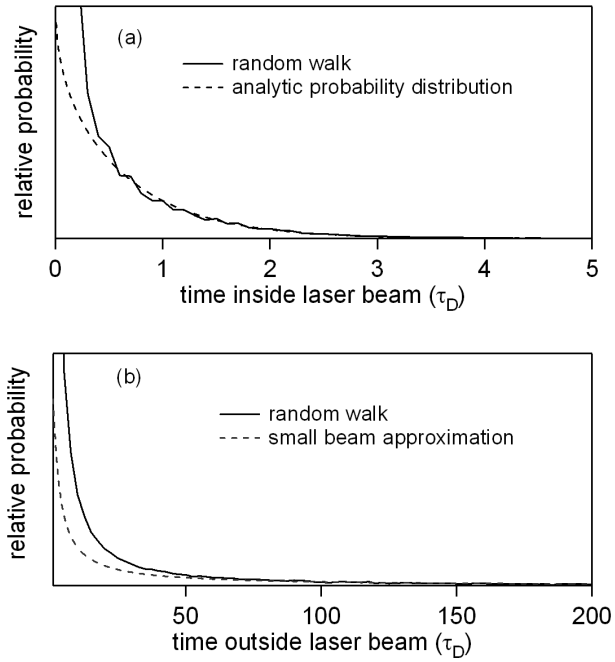

Fig. 5. Probability distributions of times (a) in the beam and (b) out of the beam in units of $\tau_D = a^2/4D$ with a ratio of cell diameter to step-like beam diameter, $d/a = 30$. The dashed lines are calculated from Eqs. (3) and (4) while the solid lines are numerical evaluations of two-dimensional random walks. At long times these calculations agree. However, at short times, the numerical evaluations show much larger (but finite) probability than predicted by the analytical model which underestimates the number of atoms leaving the beam at short times.

where J_1 is the first Bessel function of the first kind. The dashed line in Figure 5b shows $P_{\rm out}(\tilde{t}_{\rm out})$ for $d/a = 30$, where $\tilde{t}_{\rm out} = t/\tau_D$ for the small beam approximation. Note that $P_{\rm out}(\tilde{t}_{\rm out})$ is a function of d/a, the ratio of the cell radius to the beam radius (Fig. 1a). Larger ratios of d/a (smaller beams) lead to larger values of $P_{\rm out}(\tilde{t}_{\rm out})$ and thus to larger mean times outside the beam. For beam sizes small compared to the vapor cell size, atoms spend a majority of their time outside of the laser beam, which can accentuate the spectral narrowing effects of diffusion-induced Ramsey narrowing. This trend saturates when the mean diffusion time to the cell wall becomes comparable to $1/\Gamma_0$ — the ground state coherence time due to mechanisms other than wall collisions — since in this limit, many atoms return to the beam after such long periods in the dark that they have lost ground state coherence.

We also calculated $P_{\rm in}(\tilde{t}_{\rm in})$ and $P_{\rm out}(\tilde{t}_{\rm out})$ numerically for random walk atomic motion and initial and final conditions that have atoms start and end on the laser boundary. A two-dimensional random walk was evaluated by placing a particle on a grid and repeatedly moving it in random directions on the grid. The time of each crossing of the boundary between the laser beam and the dark region of the vapor cell by the particle was tagged. By histogramming the time differences corresponding to the times during which the particle was in or out of the laser beam, the distributions were assembled. The results of these lengthy numerical calculations for $P_{\rm in}(\tilde{t}_{\rm in})$ and $P_{\rm out}(\tilde{t}_{\rm out})$ are given by the solid lines of Fig. 5. Further detail is provided in Sec. 4.

Compared to the numerical calculations, we find that the approximate analytical expressions

#97131 - $15.00 USD Received 6 Jun 2008; revised 1 Aug 2008; accepted 4 Aug 2008; published 26 Aug 2008

for $P_{\rm in}(\tilde{t}_{\rm in})$ [Eq. (3)] and $P_{\rm out}(\tilde{t}_{\rm out})$ [Eq. (4)] underestimate short time departures from and returns to the beam, respectively. Additionally, we assume a step-like laser beam profile, rather than a more realistic profile such as a Gaussian. Therefore, the behavior of atoms close to the boundary is not well modeled. However, at low laser intensities and/or small beam diameters, such that the optical pumping time is long compared to the time to diffuse through the beam ($\alpha^{-1}\tau_D << 1$), we find that the detail of the beam profile is unimportant and may be accounted for in the repeated interaction model through small, consistent adjustments of beam diameter and intensity. With these small adjustments we find equivalent calculated EIT lineshapes for the analytical and numerical versions of the $P_{\rm in}(\tilde{t}_{\rm in})$ and $P_{\rm out}(\tilde{t}_{\rm out})$ distributions. See Secs. 3 and 4.

2.3. Integration over all Ramsey sequences

Each atom in a vapor cell with buffer gas has a unique, stochastic history of times spent in and out of the laser beam. Therefore, in the repeated interaction model the full EIT lineshape is found by integrating Eq. (1), which gives the probe field absorption/transmission spectrum for a specific Ramsey sequence, over the distributions of times spent in and out of the beam [$P_{\rm in}$ and $P_{\rm out}$ given by Eqs. (3) and (4)]. To simplify evaluation of this integration we approximate the infinite sums in Eqs. (3) and (4) by fitting these functions to a finite sum of exponentials.

Examples of calculated EIT lineshapes that result from the repeated interaction model are shown by dashed lines in Fig. 6. Characteristic features of these generally non-Lorentzian lineshapes are a sharp central peak and a broad pedestal. The sharp central feature arises because only the central Ramsey fringe near zero two-photon detuning ($\Delta \approx 0$) adds coherently for most Ramsey sequences. The width of the sharp central peak is limited by the ground-state atomic decoherence rate, determined by atomic collisions, field gradients, collisions with the cell walls, etc. The broad pedestal is from the incoherent sum of fringes off two-photon resonance for all atoms, therefore its width is associated with the single pass interaction time and is subject to power broadening.

In general, the repeated interaction model indicates that the non-Lorentzian character of the EIT lineshape is enhanced in the limits of: weak laser power such that optical pumping is slow compared to atomic diffusion out of the laser beam ($\Omega << \tau_D^{-1}$); low buffer gas pressure and small laser beam size such that atomic diffusion out of the laser beam is fast compared to ground state decoherence ($\Gamma_0 << \tau_D^{-1}$); and small laser beam radius compared to cell size ($a << d$) such that atomic coherence can have long evolution in the dark without wall collisions. In these limits (see Fig. 6a) the sharp central peak is largely insensitive to power broadening because it results from the long evolution of atomic coherence in the dark. However, at high laser intensity the calculated central peak loses contrast relative to the broad pedestal because a sufficiently large optical pumping rate α [see eq. (11)] drives to zero all terms in Eq. (1) proportional to $\exp(-\alpha t_i)$, leaving a Lorentzian lineshape due to the lowest-order diffusion mode with a power-broadened width of $\Gamma = \alpha + \Gamma_0$. At moderate laser intensities, reduced but non-zero Ramsey fringe contrast results in moderate narrowing of the EIT lineshape center (see Fig. 6b). Similarly, as shown in Fig. 6c, the calculated contrast of the sharp central peak is reduced at higher buffer gas pressure (and hence slower atomic diffusion and greater τ_D) for two reasons: (i) longer residence time in the beam compared to a fixed optical pumping rate takes the system toward the regime of equilibrium EIT, in which the atomic ground state populations and coherence approach equilibrium with the optical fields (and the associated Lorentzian EIT lineshape) during a single atomic residence time in the laser beam; and (ii) slower diffusion decreases the fraction of atoms that undergo coherent evolution in the dark and return to the laser beam before decohering.

#97131 - $15.00 USD Received 6 Jun 2008; revised 1 Aug 2008; accepted 4 Aug 2008; published 26 Aug 2008

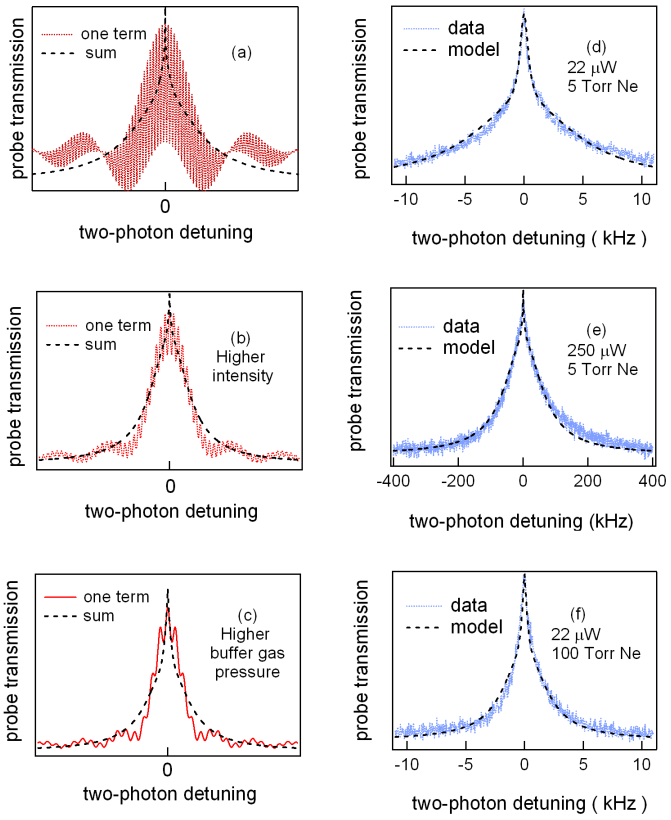

Fig. 6. Left column: decrease of Ramsey fringe contrast under high buffer gas pressure or laser intensity leads to a reduction in the sharp, central EIT feature. Solid curves are Ramsey-EIT resonances calculated from a single Ramsey sequence. Dashed curves are weighted averages over all histories. Right column: results of repeated interaction model compared to experimental data for various buffer gas pressures and laser intensities. Dashed curves are model fits and are the same for both the left and right column.

#97131 - $15.00 USD Received 6 Jun 2008; revised 1 Aug 2008; accepted 4 Aug 2008; published 26 Aug 2008

3. Comparison with experiment

As first demonstrated in our previous work [4], calculated EIT lineshapes from the repeated interaction model agree well with experimental observations. For example, the right side of Fig. 6 shows fitted lineshapes from the repeated interaction model with data for three regimes of experimental parameters. The EIT measurements were performed in optically thin Rb vapor to avoid density narrowing effects [21], and with a relatively small laser beam (0.8 mm separation between half-intensity points) in a vapor cell of 2.5 cm diameter. Experimental details are provided in Refs. [12, 4]. At low buffer gas pressure and low laser intensity (Fig. 6d) both the measured and repeated-interaction-model lineshapes exhibit clear signatures of diffusion-induced Ramsey narrowing, with a sharp central feature that is spectrally much narrower than expected from transit-time broadening associated with the lowest order diffusion mode. At high laser intensity (Fig. 6e) or high buffer gas pressure (Fig. 6f) the narrow central peak becomes less prominent relative to the broad pedestal; and the overall lineshape is somewhat more Lorentzian.

The repeated interaction model described above omits several processes that can affect EIT peak amplitude and off-resonant transmission, including additional ground and excited states [22], residual absorption of the probe and drive fields along the vapor cell axis, and radiation trapping. Therefore, in fits of the repeated interaction model to measured EIT lineshapes, we used the peak transmission amplitude and off-resonant transmission as free parameters. We accounted for both pressure-broadening of the electronic excited state and Doppler-broadening of the one-photon ground/excited-state transition by scaling the Rabi frequencies Ω_D and Ω_P with an empirical fitting-parameter that varied only with buffer gas pressure. Also, as noted above, we employed small, consistent adjustments of the laser beam diameter and intensity to correct for effects of the step-like beam profile assumed in the repeated interaction model. For example, the EIT data shown in Figs. 2 and 6 was acquired with a laser beam diameter measured to be 0.8 mm, as determined from the 1/e intensity positions across the approximately Gaussian laser profile. We found that an effective beam diameter fixed at 0.96 mm optimized fits of the repeated interaction model for all these EIT lineshapes.

For very high buffer gas pressure and high laser intensity, we found that the repeated interaction model predicts a less sharp central feature than that observed in experiment. We attribute this discrepancy to tighter confinement of the atoms by the high-pressure buffer gas and strong optical pumping by the large laser intensity. This combination of factors allows atoms to reach equilibrium with local laser fields, which accentuates the significance of details of the transverse laser beam profile [17, 18]. (See Sec. 4 and Fig. 8b.)

4. Comparison with numerical calculations

We also compared predictions of the repeated interaction model to numerical solutions of the equations of motion in the presence of diffusion. We found the steady-state solution by performing successive over-relaxation [23] for the equations of motion of the Bloch vector. The Bloch vector, $\vec{R}$, represents the populations and coherence of the two ground states of the three level Λ-system as an effective two-level system [see appendix and esp. Eq. (9)]. The equations of motion in the presence of diffusion may be written as

$$-D\nabla^2\vec{R}(r) = \begin{bmatrix} -(\alpha(r)+\Gamma_0) & -\beta'(r) & 0 \\ \beta'(r) & -(\alpha(r)+\Gamma_0) & \Delta\sin(2\theta) \\ 0 & -\Delta\sin(2\theta) & -(\alpha(r)+\Gamma_0) \end{bmatrix} \vec{R}(r) + \begin{bmatrix} 0 \\ 0 \\ \alpha(r) \end{bmatrix}, \quad (5)$$

where $\beta'(r) = \frac{\Omega^2(r)\delta}{\gamma^2+4\delta^2} - \Delta\cos(2\theta)$, $\alpha(r) = \frac{\Omega^2(r)\gamma}{2(\gamma^2+4\delta^2)}$, $\Omega^2(r) = \Omega_P^2(r) + \Omega_D^2(r)$, $\sin\theta = \Omega_P/\Omega$ [see Eq. (9)], and D is the diffusion coefficient. The optical coherence and thus the transmitted

#97131 - $15.00 USD Received 6 Jun 2008; revised 1 Aug 2008; accepted 4 Aug 2008; published 26 Aug 2008

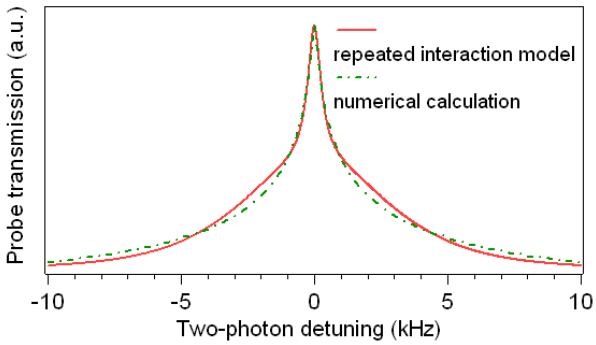

Fig. 7. Comparison between repeated interaction model (red solid line) and pure numerical calculation (green dashed line). Red solid line: prediction from the repeated interaction model for a step-like laser beam with 0.96 mm diameter and 100 Hz FWHM groundstate linewidth. This is the same curve as the "model evaluation" in Fig. 2. Green dashed line: prediction from the numerical calculation for a 0.8 mm diameter step-like beam and 200 Hz FWHM groundstate linewidth. Common parameters: Rabi frequency of $\Omega_D = 2\pi \times 95$kHz , cell diameter $2d = 2.54$ cm; excited state full width $\gamma/\pi = 100$ MHz; 30 cm^2/s Rb diffusion coefficient. A smaller ground state coherence decay rate is used in the repeated interaction model to match the pure numerical calculation because the former underestimates short interaction times (see Fig. 5) hence overestimating the linewidth of the Ramsey-EIT envelope (see Fig. 4).

intensity can then be calculated from Eq. (15) of the appendix.

Equivalent approximations regarding the internal degrees of freedom are made in this calculation as in the repeated interaction model. We assume an optically-thin medium of three-level atoms in which the optical fields are weak enough that the excited state may be adiabatically eliminated. However, we numerically solve the diffusion equation exactly in two-dimensions rather than invoking the approximations of the repeated interaction model. Diffusion induced Ramsey narrowing is evident in these numerical calculations and is in good agreement with both the repeated interaction model and experimental data (Fig. 7). While these calculations are free from the approximations of the repeated interaction model described above, they provide less intuition and are calculationally intensive [24].

Nevertheless, the relaxation calculations are useful for comparing results for step-like laser beams and Gaussian profile beams. For laser powers such that the optical pumping rate, Ω^2/γ is slow compared to the rate associated with the lowest order diffusion mode, $1/\tau_D = 4D/a^2$, the lineshapes are identical for the two types of beam profiles (Fig. 8a). This result is unsurprising as atoms under this condition typically sample the full profile of the laser beam before reaching equilibrium. However, as the beam power is increased such that optical pumping is fast compared to the rate of diffusion out of the laser beam, the laser profile begins to affect the resonance lineshape (Fig. 8b). Additionally, the lineshapes change from the low-power lineshapes and begin to resemble the peaked arctangent shape found previously in a model designed to treat this fast optical pumping limit [18].

5. Conclusions

In conclusion, we provided a detailed description of the repeated interaction model of diffusion-induced Ramsey narrowing: an intuitive analytical model based on a weighted average of distinct atomic histories arising from the diffusion of coherence in and out of an interaction region,

#97131 - $15.00 USD Received 6 Jun 2008; revised 1 Aug 2008; accepted 4 Aug 2008; published 26 Aug 2008

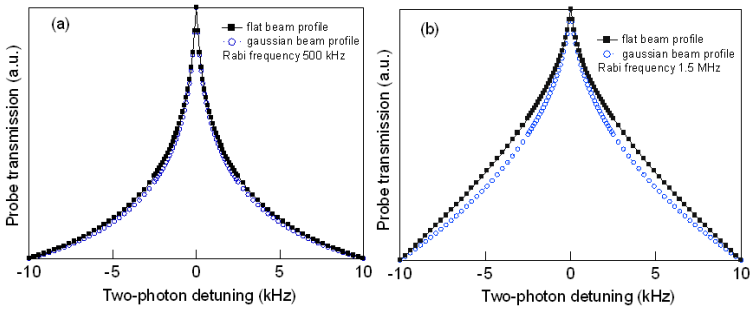

Fig. 8. Numerical integration of the steady-state solution to the Bloch equations in the presence of diffusion shown for a transverse laser profile that is step-like (filled squares) and Gaussian (open circles) with mean Rabi frequencies of (a) $\Omega_D = 2\pi \times 95$ kHz and (b) $2\pi \times 1.5$ MHz. Common parameters: beam diameter $2a = 0.8$ mm; cell diameter $2d = 2.54$ cm; 300×300 grid; excited state full width $\gamma/\pi = 100$ MHz; ground state full width $\Gamma_0/\pi = 100$ Hz.

such as a laser beam. We compared the predictions of this model both to measurements on EIT in warm Rb vapor and numerical calculations of the Bloch equations in the presence of atomic diffusion. The repeated interaction model and diffusion-induced Ramsey narrowing are relevant to spectroscopy, quantum optics, and emerging solid-state applications [25, 26, 27] based on long-lived coherences. They are particularly relevant to atomic vapor cells with buffer gas, as commonly used in frequency standards, EIT and slow light, and nonlinear magneto-optic rotation experiments. For precision spectroscopy, the resonance center is often determined via a modulation-induced dispersive-like response, which is equivalent to the derivative of the transmission. If the lineshape has the sharp, central feature of diffusion-induced Ramsey narrowing, then the measured linewidth will typically be set by the width of the central narrow peak rather than the much broader width of the transmission spectra [12]. Also, this narrow peak width is relatively immune to power broadening because atoms spend a significant fraction of their intrinsic coherence time in the dark outside the laser beam. In EIT and slow light experiments, the non-Lorentzian lineshapes resulting from diffusion-induced Ramsey narrowing can lead to a smaller distortion-free frequency bandwidth for probe pulse propagation than would be expected from a Lorentzian lineshape.

We are grateful to F. Canè, M. Hohensee, C. Hancox, M. Fleischhauer, A. Glenday, M. Klein, D. Chang, Y. Li, J. Vanier, and A. S. Zibrov for useful discussions. This work was supported by ONR, DARPA, and the Smithsonian Institution.

Appendix : Evolution of atomic density matrix for a Ramsey sequence

The dark state basis of the system consisting of a three-level Λ atom and the two laser fields, $\{|-\rangle, |+\rangle, |e\rangle\}$ (see Fig. 3) can be written as

$$|-\rangle = \cos\theta|\tilde{a}\rangle - \sin\theta|\tilde{b}\rangle, \text{ and } |+\rangle = \sin\theta|\tilde{a}\rangle + \cos\theta|\tilde{b}\rangle \tag{6}$$

where $\sin\theta = \Omega_P/\Omega$, $\cos\theta = \Omega_D/\Omega$, $\Omega^2 = \Omega_P^2 + \Omega_D^2$, and $|\tilde{a}\rangle = |a\rangle e^{-i\omega_p t}$ and $|\tilde{b}\rangle = |b\rangle e^{-i\omega_d t}$ are the ground state basis in the rotating frame. The density matrix equation in this dark state basis is [16]

$$\dot{\rho} = \frac{i}{\hbar}\left(\rho H^\dagger - H\rho\right) + \left(\rho_{ee}\frac{\gamma}{2} + \frac{\Gamma_0}{2}\right)\begin{bmatrix} 1 & 0 & 0 \\ 0 & 1 & 0 \\ 0 & 0 & 0 \end{bmatrix}, \tag{7}$$

#97131 - $15.00 USD Received 6 Jun 2008; revised 1 Aug 2008; accepted 4 Aug 2008; published 26 Aug 2008

where the Hamiltonian, H, is given by

$$H = \frac{\hbar}{2}\begin{bmatrix} C_2\Delta - i\Gamma_0 & S_2\Delta & 0 \\ S_2\Delta & -C_2\Delta - i\Gamma_0 & -\Omega \\ 0 & -\Omega & -2\delta - i\gamma \end{bmatrix} \tag{8}$$

with $C_2 = \cos 2\theta$, $S_2 = \sin 2\theta$, Δ the two-photon detuning, and δ the one-photon detuning of both fields (see Fig. 3). If $S_2\Delta$ and $\Omega \ll \gamma$, then the excited state adiabatically follows the ground state, reducing the system to a two-level system with new basis $\{|-\rangle, |+\rangle_d\}$ where $|+\rangle_d = |+\rangle + \frac{i\Omega}{\gamma - i2\delta}|e\rangle$ (following Ref. [16]). Neglecting terms higher than first order in Ω/γ allows us to represent the system with a Bloch vector $\vec{R}$ given by [16]: $R_1 = \rho_{+-} + \rho_{-+}$, $R_2 = i(\rho_{+-} - \rho_{-+})$, and $R_3 = \rho_{--} - \rho_{++}$, and an equation of motion:

$$\dot{\vec{R}} = \begin{bmatrix} -(\alpha+\Gamma_0) & -\beta' & 0 \\ \beta' & -(\alpha+\Gamma_0) & S_2\Delta \\ 0 & -S_2\Delta & -(\alpha+\Gamma_0) \end{bmatrix}\vec{R} + \begin{bmatrix} 0 \\ 0 \\ \alpha \end{bmatrix}, \tag{9}$$

with

$$\beta' = \frac{\Omega^2\delta}{\gamma^2 + 4\delta^2} - C_2\Delta \tag{10}$$

and

$$\alpha = \frac{\Omega^2\gamma}{2(\gamma^2 + 4\delta^2)}. \tag{11}$$

In Eq. (9), $S_2\Delta$ is analogous to the Rabi frequency and β' to the detuning.

Optical pumping at a rate α also acts as a decoherence mechanism for the two-photon resonance, leading to power broadening. As pointed out in [16], Eq. (9) also represents the rotation of the Bloch vector, $\vec{R}$, about the axis $\vec{Q} = -S_2\Delta\vec{e}_1 + \beta'\vec{e}_3$ at a rate $\Omega_{\text{eff}} = \sqrt{(S_2\Delta)^2 + \beta'^2}$. The solution of Eq. (9) is

$$\vec{R}(t) = \vec{R}_s + e^{-(\alpha+\Gamma_0)t}P^{-1}e^{\Lambda t}P(\vec{R}(0) - \vec{R}_s) \tag{12}$$

where $\vec{R}_s$ is the steady state solution of Eq. (9), $\vec{R}(0)$ is the initial value (which is zero if the system starts without coherence and with equal populations in the ground states), and

$$\Lambda = \begin{bmatrix} 0 & 0 & 0 \\ 0 & -i\Omega_{\text{eff}} & 0 \\ 0 & 0 & i\Omega_{\text{eff}} \end{bmatrix} \text{ and } P^{-1} = \begin{bmatrix} -S_2\Delta & \beta' & \beta' \\ 0 & i\Omega_{\text{eff}} & -i\Omega_{\text{eff}} \\ \beta' & S_2\Delta & S_2\Delta \end{bmatrix}. \tag{13}$$

The time to reach steady state is $\sim 1/(\alpha+\Gamma_0)$ [see Eq. (12)] which is also the inverse of the steady state EIT linewidth when not limited by transit time broadening.

Using Eq. (12), we can derive an atom's polarization in response to a Ramsey pulse sequence. Applying Eq. (12) to a sequence $[t_1, t_2, t_3]$ shown in Fig. 1b, and noting that $\Omega_{\text{eff}} = \Delta$, when atoms are outside of the laser beam, $\vec{R}$ at the end of the sequence is

$$\begin{aligned} \vec{R}(t_1,t_2,t_3) &= \{1 - e^{-(\alpha+\Gamma_0)t_3}P^{-1}e^{\Lambda t_3}P \\ &+ e^{-(\alpha+\Gamma_0)t_3 - \Gamma_0 t_2}P^{-1}e^{\Lambda(t_3+t_2)}P(1 - e^{-(\alpha+\Gamma_0)t_1}P^{-1}e^{\Lambda t_1}P)\}\vec{R}_s \end{aligned} \tag{14}$$

where the first row of the right hand side represents the polarization newly obtained during t_3; and the second row, which is responsible for the Ramsey fringes, describes the polarization that is obtained during t_1 and then under phase evolution and amplitude loss during t_2 and t_3. The decay rate of the Bloch vector associated with a time in the beam is $\alpha + \Gamma_0$, while outside the beam the rate is Γ_0.

#97131 - $15.00 USD Received 6 Jun 2008; revised 1 Aug 2008; accepted 4 Aug 2008; published 26 Aug 2008

Atomic polarization interacting with the probe field can be written in terms of $\vec{R}$ as

$$\rho_{\tilde{e}\tilde{a}} = \frac{i}{2(\gamma - i2\delta)}\{\Omega_D(R_1 - iR_2) + \Omega_P(1 - R_3)\}, \tag{15}$$

and the field absorption coefficient is expressed as $-\frac{3}{8\pi}n\lambda^2\gamma_r Im(\frac{\rho_{\tilde{e}\tilde{a}}}{\Omega_P})$, where n is atomic density, λ the optical wavelength, and γ_r the radiative decay rate of the excited state.

For zero one-photon detuning and a small ratio of probe to pump Rabi frequency ($\sin\theta \approx \theta$), the imaginary part of $\rho_{\tilde{e}\tilde{a}}$ has a relatively simple form:

$$\begin{aligned}\frac{\mathrm{Im}\,(\rho_{\tilde{e}\tilde{a}})}{\Omega_P} = & \\ & \frac{\alpha_D}{(\Delta^2+\Gamma^2)(\gamma^2+\Delta^2)} \cdot \mathrm{Re}\left\{\left[\gamma\Gamma - \Delta^2 + i\Delta(\gamma+\Gamma)\right] \cdot \right. \\ & \left.\left(-1 + e^{-t_3(\Gamma - i\Delta)} - e^{-t_3(\Gamma-i\Delta)-t_2(\Gamma_0-i\Delta)} + e^{-(t_1+t_3)(\Gamma-i\Delta)-t_2(\Gamma_0-i\Delta)} + \cdots\right)\right\} \\ & -\frac{\alpha_D\gamma}{2\Gamma(\gamma^2+\Delta^2)} \cdot (-1 + e^{-t_3\Gamma} - e^{-t_3\Gamma - t_2\Gamma_0} + e^{-(t_1+t_3)\Gamma - t_2\Gamma_0} + \cdots) + \\ & \frac{\gamma}{2(\gamma^2+\Delta^2)}\end{aligned} \tag{16}$$

where $\Gamma = \alpha_D + \Gamma_0$, $\alpha_D = \Omega_D^2/2\gamma$, and "$\cdots$" represents terms accounting for more than one diffusive return to the laser beam. Each return adds two terms similar to those in the parentheses. Further interpretation of this equation is provided in sec. 2.

#97131 - $15.00 USD Received 6 Jun 2008; revised 1 Aug 2008; accepted 4 Aug 2008; published 26 Aug 2008